JOURNAL OF OPTOELECTRONICS AND ADVANCED MATERIALS Vol. 10, No. 10, October 2008, p. 2578 - 2583

Preparation and characterization of ZnO thin films deposited by sol-gel spin coating method

S. ILICAN*, Y. CAGLAR, M. CAGLAR
Department of Physics, Faculty of Science, Anadolu University, 26470 Eskisehir, Turkey

ZnO thin films have been deposited onto the glass substrates by the sol-gel spin coating method at different chuck rotation rates. This method was used for the preparation of thin films of the important semiconductors II-VI. The effect of deposition parameters on the structural, optical and electrical properties of the ZnO thin films was investigated. Zinc acetate dehydrate, 2-methoxethanol and monoethanolamine (MEA) were used as a starting material, solvent and stabilizer, respectively. Thermogravimetric analysis (TGA) of the dried gel showed that weight loss continued until 300 ^oC. The crystal structure and orientation of the ZnO thin films were investigated by X-ray diffraction (XRD) patterns. The grain size of the films was calculated using the Scherrer formula. The optical absorbance and transmittance measurements were recorded by using a double beam spectrophotometer with an integrating sphere in the wavelength range 190-900 nm. The optical absorption studies reveal that the transition is direct band gap energy. The optical band gaps and Urbach energies of the thin films were determined. The *I-V* plots of the ZnO thin films were carried out in dark and under UV-illumination. The obtained ZnO thin films can be used as a photovoltaic material.

(Received February 14, 2008; accepted August 14, 2008)

Keywords: ZnO, sol-gel spin coating, crystal structure, optical band gap, *I-V* characteristics.

1. Introduction

ZnO thin film is one of the II-VI compound semiconductors and is composed of hexagonal wurtzite crystal structure. ZnO thin film presents investigating optical, acoustical and electrical properties which meet extent applications in the fields of electronics, optoelectronics and sensors. ZnO thin film is applied to the transparent conductive film and the solar cell window because of the high optical transmittance in the visible region. Studies on the application of ZnO thin film to the surface acoustic wave (SAW) device and film bulk acoustic resonator (FBAR) filter are being made, because of its excellent piezoelectric properties [1–5].

The ZnO thin film is prepared using various methods such as spray pyrolysis, sputtering, sol-gel spin coating, pulsed laser deposition (PLD), chemical vapor deposition (CVD) [6–10]. In spite of few studies regarding to the sol-gel method, the sol-gel method has some merits, such as the easy control of chemical components, and fabrication of thin film at a low cost to investigate structure and optical properties of ZnO thin films.

In previous work we reported on the ZnO thin films deposited by spray pyrilisis [11] and effect of indium on the properties of zinc oxide films [12,13].

In this work, the effect of chuck rotation rate on the structural, optical and electrical properties of ZnO thin films is reported.

2. Experimental

ZnO thin films were deposited by sol-gel spin coating method onto glass substrates. Zinc acetate dehydrate, 2-methoxethanol and monoethanolamine (MEA) were used as a starting material, solvent and stabilizer, respectively. The molar ratio of MEA to zinc acetate dehydrate was maintained at 1.0 and the concentration of zinc acetate was 0.35 M. The glass substrate was precleaned detergent, and then cleaned in methanol and acetone for 10 min each by using a Bandelin Sonorex RK100 ultrasonic cleaner and then cleaned with deionized water and dried. The coating solution was dropped onto glass substrate, which was rotated at 3000 rpm, 4000 rpm and 5000 rpm for 30 s by using LAURELL WS-400B-6NPP/LITE spin coater. After depositing by spin coating, the film was dried at 300 ^oC for 10 min in a furnace to evaporate the solvent and remove organic residuals. The procedures from coating to drying were repeated ten times. The film was then inserted into a tube furnace and annealed in air at 550 ^oC for 1 h.

Fig. 1 shows the flow chart which is showing the procedure for preparing ZnO thin films. The thicknesses of the films were determined with Mettler Toledo MX5 microbalance by using weighing method and found to be between 140 nm and 180 nm. The film thickness changes inversely with chuck rotation rate. TGA and DTA curves of the dried ZnO gel were recorded using a Setaram Labsys TG/DTA with ca. 15 mg of sample and a scanning rate of 5° min^-1 under argon between about 25 ^oC - 800 ^oC. X-ray diffraction patterns were obtained with a RIGAKU RINT 2200 Series X-Ray Automatic Diffractometer using the CuK_α radiations (λ=1.54059 Å) in the range of 2θ between 20° and 60°. The diffractometer reflection was taken at room temperature. The optical measurement of the film was carried out at room temperature using Shimadzu UV-VIS 2450 spectrophotometer with integrating sphere in the wavelength range from 190 to

900 nm. The conductivity types of the films were verified by the hot probe method. The current–voltage (*I–V*) measurements in dark and under illumination conditions were performed using KEITHLEY 2400 sourcemeter and GPIB data transfer card for *I-V* measurements. The light source consisting of a UV-lamp was used for *I–V* measurements under illumination.

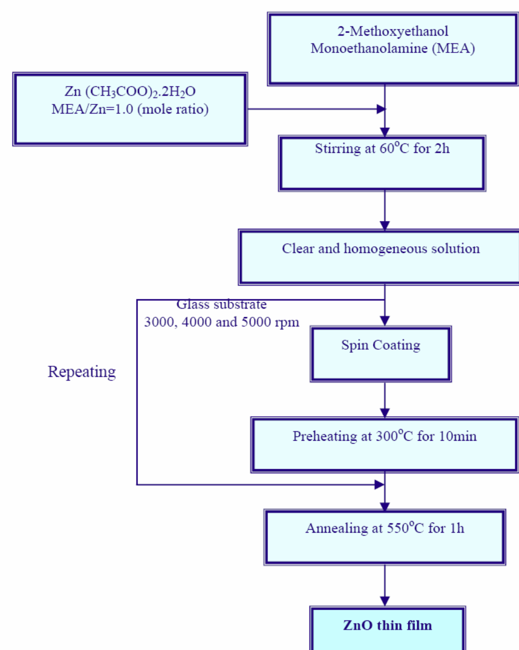

Fig. 1. The flow chart showing the procedure for preparing ZnO thin films.

3. Results and Discussion

3.1. Thermal analysis of the dried ZnO gel

The thermal behaviours of dried ZnO gel have been investigated by differential thermal analysis (DTA) and thermogravimetric analysis (TGA). The TG-DTA result is shown in Fig. 2.

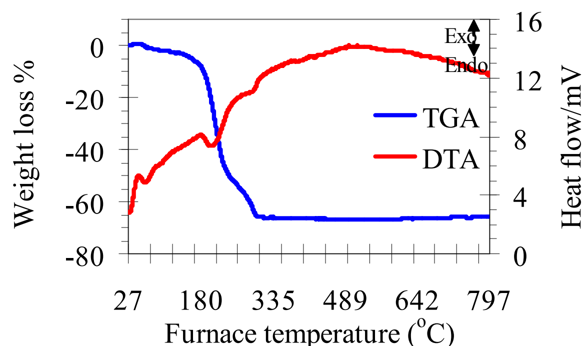

Fig. 2. TGA and DTA analysis of dried ZnO gel.

Two weight losses were observed at about 50-100 °C and 175-300 °C in the TG curve. The first weight loss is due to the evaporation of water and 2-methoxyethanol. The second weight loss is caused by the decomposition of residual organics and MEA. Three endothermic peak was found at 63 °C, 202 °C and 291 °C, respectively. These peaks were accompanied by the weight loss mentioned above. It is observed that there is no weight loss after the about 300 °C. So, the preheating temperature was selected 300 °C.

3.2. Crystal structure of the ZnO thin films

The crystal structure and orientation of the ZnO thin films were investigated by X-ray diffraction (XRD) patterns. The XRD spectra for ZnO thin films shown in Fig. 3.

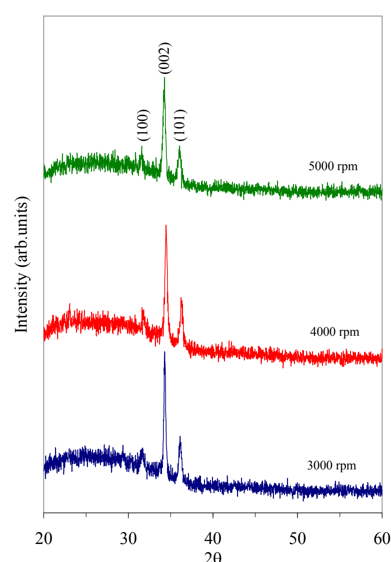

Fig. 3. X-ray diffraction spectra of ZnO thin films.

XRD diffraction peaks belonging to (100), (002), and (101) planes were observed in all the ZnO films. Compared to powder diffraction data of zincite structure [14], the XRD patterns of all the samples indicated enhanced intensities for the peaks corresponding to (002) plane, indicating preferential orientation along the c-axis.

The full width at half maximum (FWHM) of ZnO thin films for (002) plane are given in Table 1. FWHM of thin films shows an increase with increasing chuck rotation rate. The grain size *D* of crystallites was calculated using a well-known Scherrer's Formula [15]. The dislocation density δ which represents the amount of defects in the film was determined from the formula $\delta=1/D^2$ [16]. These values are given in Table 1.

The larger *D* and smaller FWHM values indicate better crystallization of the film. It was observed that the grain size values decrease with increasing chuck rotation rate, which clearly reveals the deterioration in the crystallinity.

Table 1. The structural parameters of ZnO thin films.

	FWHM	*2θ*	*D (nm)*	*δx10^{-4} (nm)$^{-2}$*	*a/c*	*L (Å)*
3000 rpm	0.272	34.319	31.9	9.80	0.6237	1.9825
4000 rpm	0.288	34.460	30.2	10.98	0.6278	1.9835
5000 rpm	0.341	34.280	25.5	15.41	0.6253	1.9881
Ref. [11]	-	34.420	-	-	0.6242	1.9778

Dislocation densities exhibit an increasing trend with increasing chuck rotation rate, which leads to the increasing in the concentration of lattice imperfections.

Lattice constants *a* and *c* are calculated by using well-known analytical method [15]. *a/c* ratio for the thin films are given in Table 1. It can be seen that the best *a/c* ratio which agreements with JCPDS standard data belongs to ZnO film at 3000 rpm.

The Zn–O bond length *L* is given by [17]

$$L = \sqrt{\left(\frac{a^2}{3} + \left(\frac{1}{2} - u\right)^2 c^2\right)} \tag{1}$$

where the *u* parameter in the wurtzite structure is given by

$$u = \frac{a^2}{3c^2} + 0.25 \tag{2}$$

and related to *a/c* ratio. The Zn–O bond lengths are given in Table 1.

Quantitative information concerning the preferential crystal orientation can be obtained from the texture coefficient, *TC*, defined as [18],

$$TC(hkl) = \frac{I(hkl)/I_o(hkl)}{(1/n)\sum_n I(hkl)/I_o(hkl)} \tag{3}$$

where *TC(hkl)* is the texture coefficient, *I(hkl)* is the XRD intensity and n is the number of diffraction peaks considered. $I_o(hkl)$ is the intensity of the XRD reference of the randomly oriented grains. If $TC(hkl)\approx1$ for all the *(hkl)* planes considered, then the films are with a randomly oriented crystallite similar to the JCPDS reference, while values higher than 1 indicate the abundance of grains in a given *(hkl)* direction. Values $0<TC(hkl)<1$ indicate the lack of grains oriented in that direction. As *TC(hkl)* increases, the preferential growth of the crystallites in the direction perpendicular to the hkl plane is the greater. Since three diffraction peaks were used ((100), (002), (101)), the maximum value *TC(hkl)* possible is 3.

The variations of *TC(hkl)* for the peaks of the films are presented in Fig. 4.

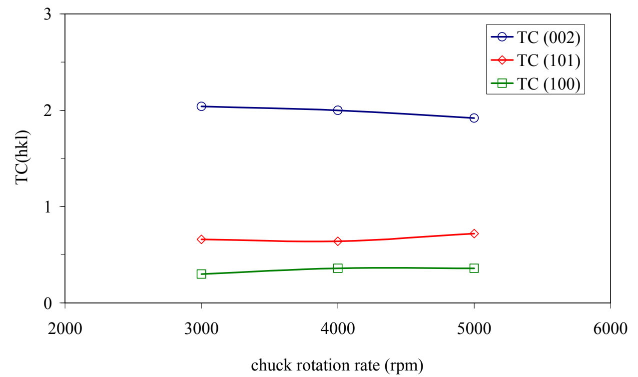

Fig. 4. Variation of TC(hkl) values of the ZnO films with chuck rotation rate.

It can be seen that the highest *TC(hkl)* was in (002) plane for all the films. The *TC*(002) values decrease with increasing chuck rotation.

3.3. Optical properties of the ZnO thin films

The optical transmittance and absorption coefficient spectra of the thin films in the UV–visible wavelength range are presented in Fig. 5.

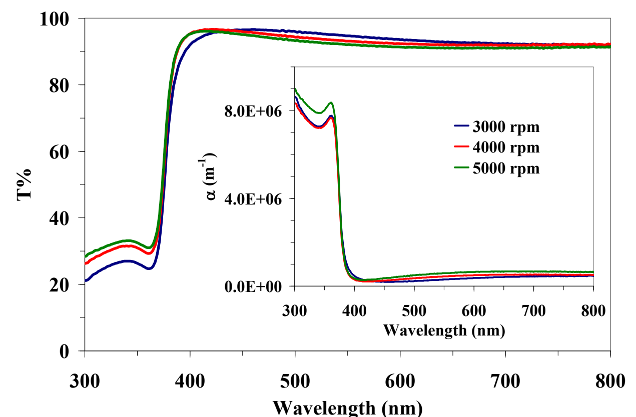

Fig. 5. Optical transmittance and absorption coefficient spectra of ZnO thin films.

It can be seen that the films have high transparency in the visible range (>92%).

The first derivative of optical transmittance spectra are presented in Fig. 6.

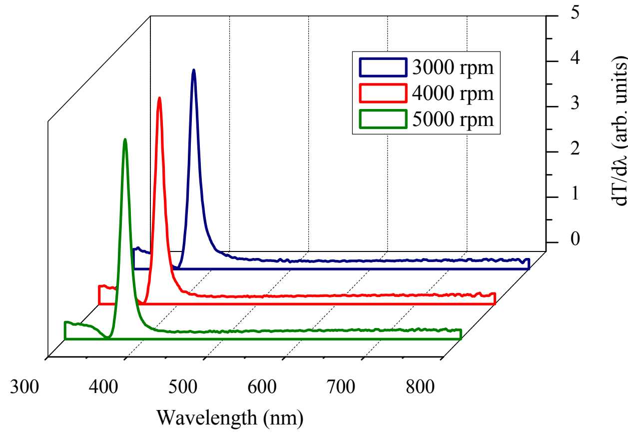

Fig. 6. First derivative (dT/dλ) plot of the transmittance spectra of the ZnO thin films.

From this Fig., the absorption wavelength values that correspond to the peaks for all of the films were 376 nm.

The optical band gap with direct transition can be calculated from the following relationship [19],

$$(\alpha h\nu) = B(h\nu - E_g)^{1/2} \quad (4)$$

where $h\nu$ is photon energy and B is a constant between 10^7 and 10^8 m^{-1}. It is well known that direct transition across the band gap is feasible between the valence and the conduction band edges in k space. In the transition process, the total energy and momentum of the electron-photon system must be conserved.

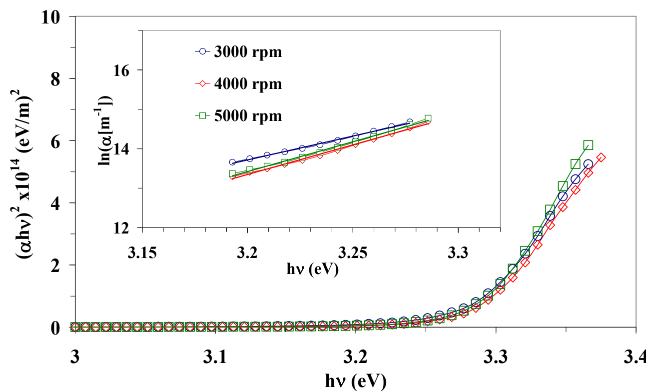

Fig. 7. The plots of $(\alpha h\upsilon)^2$ and ln(α) vs. photon energy of ZnO thin films.

Fig. 7 shows plots of $(\alpha h\nu)^2$ vs. $h\nu$. The values of the optical band gap E_g and B constant were determined and are given in Table 2. E_g values change with chuck rotation rate. The shift of absorption edge is associated with Burstein-Moss effect.

Table 2. The optical parameters of ZnO thin films.

Films	*E_g (eV)*	*E_u (meV)*	*B x10^7(m^{-1})*	*β*
3000 rpm	3.280	73	7.83	0.34
4000 rpm	3.287	55	7.98	0.45
5000 rpm	3.290	53	8.71	0.47

The absorption coefficient near the band edge shows an exponential dependence on photon energy [20]

$$\alpha = \alpha_o \exp\left[\frac{h\nu - E_I}{E_U}\right] \quad (5)$$

where E_U is the Urbach energy which corresponds to the width of the band tail, E_I and α_o are constant. Thus, a plot of $ln\alpha$ vs. $h\nu$ should be linear and Urbach energy can be obtained from the slope. Inset graph of Fig. 7 shows the variation of $ln\alpha$ vs. $h\nu$ for the ZnO thin films. Urbach energy was calculated from the reciprocal gradient of the linear portion of these curves and is shown in inset graph of Fig. 7. The calculated values are given in Table 2. Urbach energy values of the films decrease with increasing chuck rotation rate. The chuck rotation rate is responsible for the width of localized states in the optical band of the films. The E_U values change inversely with optical band gap. The dependence of the optical absorption coefficient with photon energy may arise from electronic transitions between localized states. The density of these states falls off exponentially with energy which is consistent the theory of Tauc [21]. Eq. (5) can be rewritten as,

$$\alpha = \alpha_o \exp[\frac{\beta}{kT}(E - E_I)] \quad (6)$$

where β is a called steepness parameter, which characterizes the broadening of the absorption edge due to the electron-phonon interaction or exciton–phonon interaction. If the width of the edge is related to the slope of Eq.(5), the β parameter is found as $\beta=kT/E_U$. The β values were calculated using this relationship (T=300K) and are given in Table 2. The β values suggest that the absorption edge changes with chuck rotation rate.

3.4. The I-V characteristics of the thin films

The measured dark and UV-illuminated $I–V$ characteristics are shown in Fig. 8.

Ohmic behavior and non-linear behavior in the I-V curves were observed in the ZnO thin films in dark and under UV-illumination, respectively. The current at a given voltage for the films under UV-illumination is higher than that under dark condition. This indicates that the UV-illumination increases the production of electron–hole pairs. The effect of the light on the films shows that the obtained ZnO thin films can be used as a photovoltaic material.

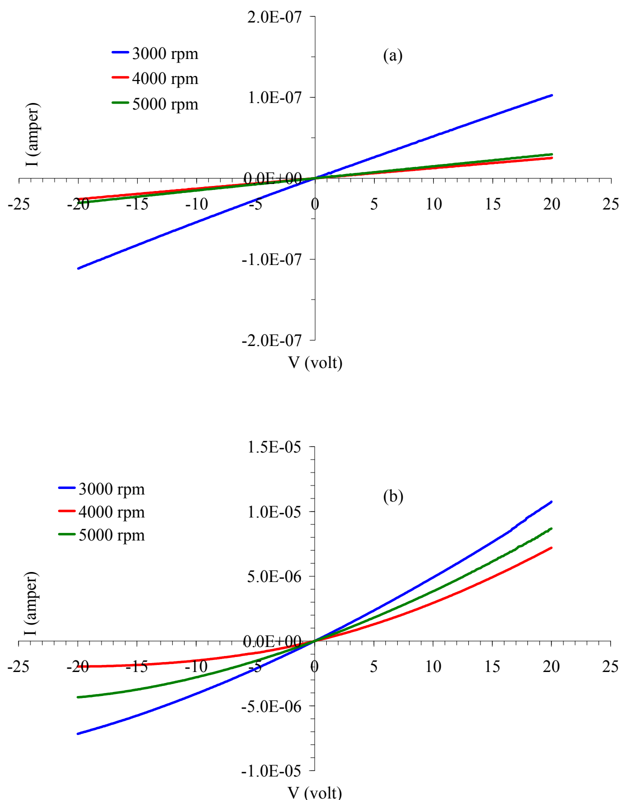

Fig. 8. I-V plots of ZnO thin films (a) in dark and (b) under UV illumination.

4. Conclusions

The structural, optical and electrical properties of sol-gel spin coated ZnO thin films have been investigated. The XRD spectra indicate that the films are of polycrystalline structure. The grain size of crystallites was found to be in the range of 25-32 nm. The values of the optical band gap and Urbach energy change with chuck rotation rate. The shift of absorption edge is associated with Burstein-Moss effect. In the visible region, all the films are highly transparent more than 92%. The I-V characteristics of the films in dark and under UV-illumination show that the sol-gel spin coated ZnO thin films are sensitive to UV-light. It is thought that because of these properties, ZnO thin films can be used as a window material in photovoltaic applications.

Acknowledgements

This work was supported by Anadolu University Commission of Scientific Research Projects under Grant No. 061039. The authors are also grateful to Anadolu University Department of Chemistry for TG-DTA measurements and Mr. Levent Ozcan for assistance in these measurements. The authors are grateful to Anadolu University Department of Materials Science and Engineering for the XRD measurements.

References

[1] A. Talbi, F. Sarry, M. Elhakiki, L. Le Brizoual, O. Elmazria, P. Nicolay, P. Alnot, Sensors and Actuators **A 128**, 78 (2006).
[2] J. J. Chen, F. Zeng, D.M. Li, J.B. Niu, F. Pan, Thin Solid Films **485**, 257 (2005).
[3] J.-B. Lee, D.-H. Cho, D.-Y. Kim, C.-K. Park, J.-S. Park, Thin Solid Films **516**, 475 (2007).
[4] A. N. Banerjee, C.K. Ghosh, K.K. Chattopadhyay, H. Minoura, A.K. Sarkar, A. Akiba, A. Kamiya, T. Endo, Thin Solid Films **496**, 112 (2006).
[5] J. Yoo, J. Lee, S. Kim, K. Yoon, I.J. Park, S.K. Dhungel, B. Karunagaran, D. Mangalaraj, J. Yi, Thin Solid Films **480**, 213 (2005).
[6] M. Caglar, Y. Caglar, S. Ilican, J. Optoelectron Adv. Mater. **8**, 1410 (2006).
[7] F. Yakuphanoglu, Y. Caglar, S. Ilican, M. Caglar, Physica B **394**, 86 (2007).
[8] Young Yi Kim, Si Woo Kang, Bo Hyun Kong, Hyung Koun Cho, Physica B **401–402**, 408 (2007).
[9] G. Srinivasana, N. Gopalakrishnanc, Y.S. Yud, R. Kesavamoorthye,J. Kumara, Superlattices and Microstructures in press.
[10] L. H. Van, M.H. Hong and J. Ding, Journal of Alloys and Compounds, **449**, 207 (2008).
[11] F. Yakuphanoglu, S. ilican, M. Caglar, Y. Caglar, J. Optoelectron. Adv. Mater. **9**(7), 2180 (2007).
[12] Y. Caglar, M. Zor, M. Caglar, S. Ilican, J. Optoelectron. Adv. Mater. **8**(5), 1867 (2006).
[13] S. Ilican, Y. Caglar, M. Caglar, B. Demirci, J. Optoelectron. Adv. Mater. **10**(10), 2592 (2008).
Joint Committee on Powder Diffraction Standards, Powder Diffraction File, card no: 36-1451.
[14] B. D. Cullity, S.R. Stock, Elements of X-Ray Diffraction, Prentice Hall, 2001, 3rd ed.
[15] G. B. Williamson, R.C. Smallman, Philos. Mag. **1**, 34 (1956).

[16] X. S. Wang, Z.C. Wu, J.F. Webb, Z.G. Liu, Applied Physics A **77**, 561 (2003).
[17] C. S. Barret, T.B. Massalski, Structure of Metals, Pergamon Press, Oxford,1980.
[18] J. I. Pankove, Optical Processes in Semiconductors, Prentice-Hall Inc., Englewoord Cliffs, NJ, 1971.
[19] F. Urbach. Phys. Rev. **92**, 1324 (1953).
[20] Tauc, J. Amorphous and Liquid Semiconductors, Plenum Press, New York 1974.

Coresponding author: silican@anadolu.edu.tr